Audio Engineering Society

Convention Paper 5641

Presented at the 113th Convention
2002 October 5–8Los Angeles, California, USA

Nonlinearity in Horn Drivers – Where the Distortion Comes From?

A. Voishvillo, AES Member[1]

[1] *Cerwin - Vega Inc., AES Sustaining member, Simi Valley, California 93065, USA*
Correspondence should be addressed to A. Voishvillo (avoishvillo@iccas.com)

ABSTRACT

Horn drivers have the worst nonlinear distortion compared to other components of professional sound systems (omitting free propagation distortion). Some of the driver's distortions can be mitigated by proper mechanical measures. However, distortions caused by nonlinear air compression and propagation are inherent to any horn driver. In this work the comparison of nonlinear distortions caused by different sources is carried through measurement and modeling. The new dynamic model of compression driver is based on the system of nonlinear differential and algebraic equations. Complex impedance of an arbitrary horn is considered by turning the impedance into a system of differential equations describing the pressure and velocity at the horn's throat. Comparison is carried out using harmonic distortion and the reaction to multitone stimulus

INTRODUCTION

A compression driver loaded by a horn is the worst source of nonlinear distortion among professional sound equipment (with exception for the free propagation distortion). A regular horn driver "harbors" various types of nonlinear distortions, the worst of them being nonlinear breakups of the diaphragm, nonlinear adiabatic compression of the air in the compression chamber, and nonlinear propagation in phasing plug and horn. Understanding basic mechanisms of nonlinear distortion in horn drivers, and the ability to predict the level of this distortion to a certain degree of accuracy, is instrumental in the design process and helps to realistically assess performance of the driver being designed without struggling for unachievable results.

Prediction of nonlinear distortion in a compression driver was attempted in a number of works where different methods of modeling were used [1] – [4]. In the course of developing a method for the current work, the models predicting reaction to steady-state tonal signal only [3] have been ruled out as well as the methods based on application of Volterra expansion [4], [5]. The former do not provide sufficient information about intermodulation distortion and cannot predict reaction to complex signals. The latter do not handle high order nonlinearity. The method using numerical solution of differential equations describing behavior of a compression driver is much more flexible because it operates with a wide class of signals such as band-limited noise, multitone stimulus, and musical signal.

Nonlinear one-dimensional model of a compression driver developed in this work considers nonlinear compression of air in compression chamber taking into account complex acoustic impedance of the horn. The impedance is approximated by a fractional-rational function, which is turned by the inverse Laplace transform into a system of approximating differential equations describing time domain relationship between sound pressure and particle velocity at the exit of compression chamber. The model also takes into account nonlinear mechanical stiffness of the suspension including nonlinear stiffness of air trapped in the back chamber, nonlinear viscous air losses in compression chamber, dependence of the voice coil inductance on displacement, frequency and current, dependence of Bl-product on voice coil displacement. The model can also take into account modulation of the Bl-product by the voice coil current and influence of turbulence in phasing plug at high levels of particle velocity in it. The model can predict compression driver's reaction to a wide class of input signals.

A one-dimensional nonlinear model of a horn considers nonlinear propagation of sound waves in the horn, taking into account the reflections of the fundamental components from the mouth. Again, the model is capable of operating with a variety of signals, including musical signal. This differentiates the model from nonlinear models dealing only with sinusoidal excitations, for example [6]. The model uses Hammerstein-Wiener "sandwich" approach [7], which is based on representing a nonlinear system by cascaded connection of linear dynamic part and nonlinear static component. A horn is split into short sections and each section is approximated by the conical linear subsection described by the matrix of the complex A-parameters, and the cylindrical nonlinear subsection, describing propagation of the plane wave along a very short distance of a particular section. Transformation of the signal by each linear section is carried out through the convolution of the signal with the pulse response of this linear section. The pulse response is calculated through the use of the inverse Fourier transform of the complex transfer function, which, in its turn, is calculated from the matrix of the A-parameters of the n-th section and the complex input acoustic impedance of the next (n+1)-th conical section. Nonlinear transformation of the signal is calculated through the use of the numerical solution of implicit equation describing the input and output velocity and pressure at the input and output of the cylindrical element. The model also handles various signals.

By using a nonlinear model of horn driver it is possible to analyze the influence of particular sources of nonlinearity (that is practically impossible using measurement of sound pressure response of horn drivers). Due to the ability of the model to process various input signals, the modeling potentially makes it possible to perform comparative subjective evaluation of various sources of nonlinearity in a horn driver and to obtain objective thresholds of audibility of nonlinear distortion in terms of such informative criteria as a reaction to multitone and incoherence function. In addition, the model developed can be eventually used as an efficient design tool. Such a tool would help not only in prediction of nonlinear distortion generated in different parts of a horn driver, but also in assessment of minimum level of nonlinear distortion that can be potentially reached, but never further minimized by any mechanical means due to the fundamental physical constraints.

COMPRESSION DRIVER

Nonlinear compression

Assuming that a compression driver has "ideal" components and is free from nonlinear distortions produced in the motor and diaphragm, still there would be inevitable distortion. This distortion would be produced in the front chamber and in the rear chamber (if it is small) due to the nonlinear compression of the air. This kind of air distortion is explained by the nonlinear relationship between the change of the volume of the chamber and the pressure in it. Distortion would be also generated in the phasing plug and horn due to the nonlinear propagation of sound waves from compression

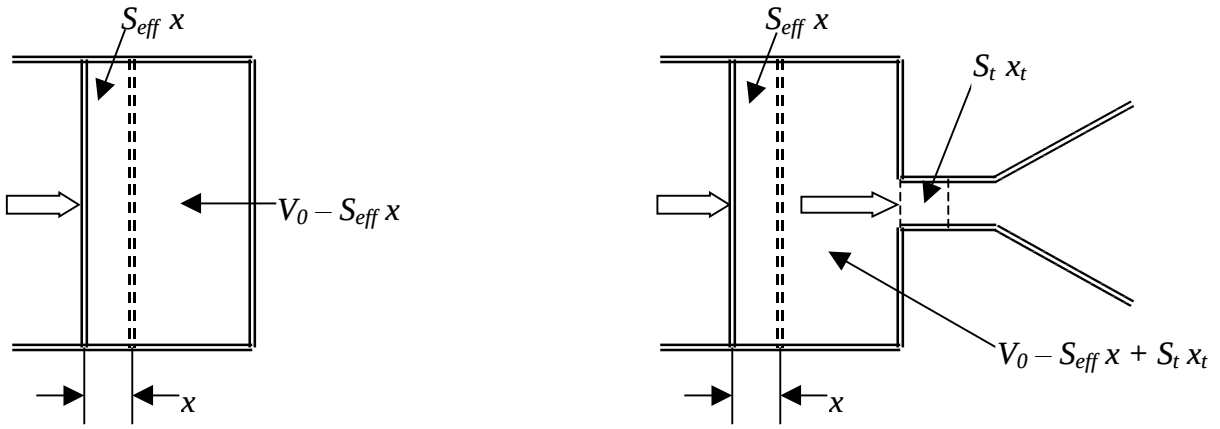

a) Sealed chamber b) Open chamber

Fig.1.1 Variation of instantaneous volume and compression of air in a sealed and open chamber.

chamber to the horn's mouth. The same kind of air distortion adversely affects sound waves propagating from the mouth of a horn to a listener. The nature of the air propagation distortion stems from two factors. The first is the nonlinear dependence of particle velocity on the relative increase in density in a sound wave. The second is the nonlinear relation between pressure and density in a sound wave. The first factor is the convective source of distortion, which determines the kinematic component of air nonlinearity. This component causes the speed of propagation of a sound wave to be dependent on the particle velocity causing faster propagation of "louder" parts of sound wave. The second factor determines the dynamic component of air nonlinearity, meaning that the air compression in a high amplitude wave does not obey Hook's law.

Also there may be distortion in the compression driver caused by the modulation of the thermoviscous losses in the thin layer of air in compression chamber due to the variation of its effective "thickness" caused by the diaphragm's movement. In addition, at a very high level of sound pressure there may be distortion in the phasing plug caused by the turbulence when the particle velocity of air exceeds critical value, which is usually expressed in terms of Reynolds number.

The nonlinear compression of air trapped in a sealed chamber is caused by the lack of linear relationship between the variation of volume and the pressure in a chamber – Fig. 1.1a. This relationship is expressed by the adiabatic equation:

$$P_0 V_0^{\gamma} = (P_0 + p)(V_0 - V)^{\gamma} \qquad (1.1)$$

where p is the sound pressure in a chamber, P_0 = 101325 Pa (194 dB SPL) is atmospheric pressure, V_0 is the steady-state volume of the chamber, $V = S_{eff}\, x$ is the instantaneous variation of the chamber's volume, S_{eff} is the effective area of the "diaphragm", x is the effective displacement of the "diaphragm", γ is the ratio of specific heat at constant pressure to that at the constant volume and has a value of 1.4 for the air.

From (1.1) it follows that the pressure p is nonlinear function of the volume variation $V = S_{eff}\, x$:

$$p = P_0 \left[\left(1 - S_{eff}\, x / V_0\right)^{-\gamma} - 1 \right] \qquad (1.2)$$

The expression (1.2) is valid for the sealed chamber, where there is no exchange of air mass between the chamber and the outside medium – Fig. 1.1a. The linear and nonlinear variation of sound pressure as a function of diaphragm's displacement is illustrated in Fig. 1.2 which depicts the difference between linear and nonlinear sound pressure in closed chamber and deterioration of the sound pressure waveform when the volume V_0 has 20 % sinusoidal variation $V = 0.2V_0 \sin\left[2\pi (xS_{eff} / 0.2V_0)\right]$.

Pronounced nonsymmetrical nonlinearity can be observed. The level of pressure's second harmonic is 12%, the third harmonic is 1.4 %. SPL of fundamental reaches 185 dB.

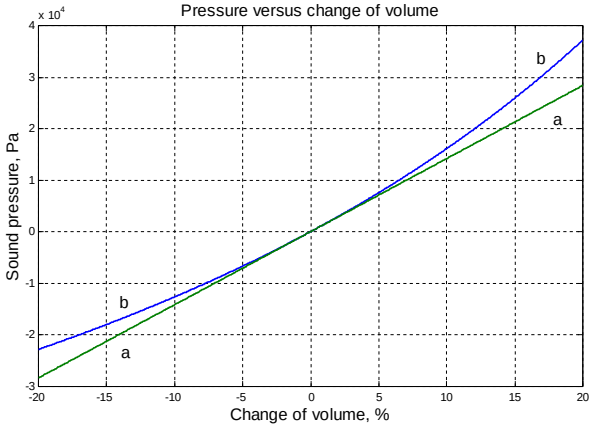

Fig. 1.2 a. Difference between linear and nonlinear air compression. The relative variation of volume is ±20 %. Dependence of sound pressure in Pa on the change of volume. Maximum SPL is 185 dB.
a – linear compression, b – nonlinear compression

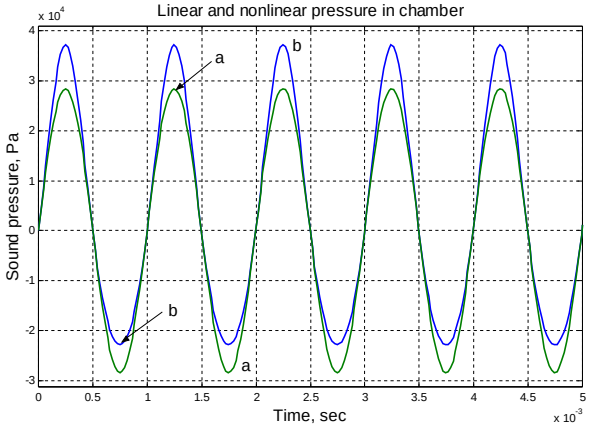

Fig. 1.2 b. The difference between linear and nonlinear air compression. The relative variation of volume is ±20 %.
a – linear compression. b – nonlinear compression. Second harmonic is 12%, third harmonic is 1.4%.

For the case of sealed chamber the air plays the role of the nonlinear spring whose stiffness $K_v(x)$ can be expressed through the dynamic relationship between the force *F* and the displacement *x*:

$$K_v(x) = \frac{dF(x)}{dx} \tag{1.3}$$

Using expression (1.2) and (1.3) and keeping in mind that the force *F* and the pressure *p* are related as $F = pS_{eff}$, an accurate expression for the stiffness of the sealed chamber can be obtained:

$$K_v(x) = S_{eff}^2 P_0 V_0^{\gamma} \gamma (V_0 - S_{eff} x)^{-\gamma-1} \tag{1.4}$$

This expression is valid for a sealed rear chamber of compression driver if the variation of volume $S_{eff} x$ is of the same order as volume V_0. If the variation of the volume is small and satisfies condition $S_{eff} x << V_0$, then the expression (1.4) takes the form:

$$K_v = \frac{S_{eff}^2 P_0 \gamma}{V_0} \tag{1.5}$$

Using the formula for the sound speed $c = \sqrt{\gamma P_0 / \rho_0}$, the well-known expression for the linear approximation of mechanical stiffness of closed air volume can be obtained:

$$K_v = \frac{S_{eff}^2 c^2 \rho_0}{V_0} \tag{1.6}$$

where ρ_0 is undisturbed density of air.

Expanding the expression (1.2) into Taylor series and truncating it after quadratic term, simplified expression for the pressure as a function of the diaphragm displacement can be obtained:

$$p(x) = \frac{c^2 \rho_0 S_{eff}}{V_0} x + \frac{c^2 \rho_0 S_{eff}}{V_0} \frac{(1+\gamma) S_{eff}}{V_0} x^2 \tag{1.7}$$

Correspondingly, the expression for the nonlinear stiffness in quadratic approximation is:

$$K_V(x) = \frac{S_{eff}^2 c^2 \rho_0}{V_0} \left[1 + \frac{(1+\gamma) S_{eff}}{V_0} x \right] \tag{1.8}$$

The compression chamber of a horn driver however is not sealed, but is open into the outside medium through the phasing plug and the horn. In this case the

instantaneous variation of volume is $V = S_{eff}\,x - S_t x_t$ rather than merely $S_{eff}\,x$ because a part of the air is displaced from the compression chamber into the phasing plug therefore changing the density of air in compression chamber. S_t is the overall area of the phasing plug's entrance, x_t is the displacement of air into the phasing plug.

Using adiabatic equation of state for an ideal gas, the sound pressure inside the compression chamber can be expressed as:

$$p = P_0\left[\left(\frac{\rho}{\rho_0}\right)^{\gamma} - 1\right] \tag{1.9}$$

where ρ is instantaneous density and ρ_0 is undisturbed density of air.

The expressions for the undisturbed and the instantaneous air densities are:

$$\rho_0 = \frac{m_v}{V_0} \tag{1.10}$$

$$\rho = \frac{m_v - \rho S_t x_t}{V_0 - S_{eff}\,x} \tag{1.11}$$

where m_v is the mass of air enclosed in equilibrium volume V_0 (see Fig. 1.1b).

Physically the implicit expression (1.11) means that the air in the chamber is compressed because the chamber's volume decreases by the volume $S_{eff}\,x$, and simultaneously, the air is "decompressed" because the part of the air's mass $\rho S_t x_t$ abandons the chamber and moves into the phasing plug. Transforming expression (1.11) into explicit form:

$$\rho(x, x_t) = \frac{m_v}{V_0 - Sx + S_t x_t} \tag{1.12}$$

and substituting (1.12) and (1.10) into (1.9) the expression for the compression chamber pressure is derived:

$$p(x, x_t) = P_0\left[\left(1 - (S_{eff}\,x - S_t x_t)/V_0\right)^{-\gamma} - 1\right] \tag{1.13}$$

Strictly speaking the volume of the air displaced in the phasing plug is a nonlinear function of displacement: $V_t(x_t) = x_t \pi \int_0^{x_t} r^2(x_t)\,dx_t$, where $r(x_t)$ is the equivalent radius of phasing plug's flare. However $r(x_t) \approx const$ for $x_t \in \{0, x_{t\max}\}$, and we assume that $V_t = S_t x_t$.

Expanding (1.13) into the Taylor series, truncating it after second order terms, and substituting $P_0\gamma = c^2\rho_0$, the following approximate expression for the chamber's sound pressure is obtained:

$$\begin{aligned} p(x, x_t) = {} & \frac{c^2\rho_0 S_{eff}}{V_0}\,x - \frac{c^2\rho_0 S_t}{V_0}\,x_t + \\ & + \frac{c^2\rho_0 S_{eff}}{V_0}\,\frac{(\gamma+1)S_{eff}}{V_0}\,x^2 - \\ & - \frac{c^2\rho_0 S_{eff}}{V_0}\,\frac{2(\gamma+1)S_t}{V_0}\,x x_t + \\ & + \frac{c^2\rho_0 S_t}{V_0}\,\frac{(\gamma+1)S_t}{V_0}\,x_t^2 \end{aligned} \tag{1.14}$$

First two right-hand terms represent the linear part of compression process, whereas the remaining three terms stand for nonlinear part of compression. Displacement of air in the phasing plug affects compression. The level of pressure depends on amplitude and phase relationship between the displacement of the diaphragm x and the displacement of air particles x_t at the entrance of the phasing plug. Having obtained expression for the force affecting the diaphragm from the "compression chamber side", we see that the stiffness is a complex function of displacements x and x_t:

$$F_c(x,x_t)=\frac{c^2\rho S_{eff}^2}{V_0}\left[1+\frac{(\gamma+1)S_{eff}}{2V_0}x\right]x- \\ -\frac{c^2\rho S_t S_{eff}}{V_0}\left[\frac{(\gamma+1)S_t}{V_0}x_t\right]x- \\ -\frac{c^2\rho S_t^2}{V_0}\left[\frac{S_{eff}}{S_t}+\frac{(\gamma+1)S_{eff}}{2V_0}x_t\right]x_t \quad (1.15)$$

First right-hand nonlinear term depends on diaphragm displacement, the second term depends on both displacements x and x_t, whereas the third nonlinear term depends only on displacement x_t. Analysis of expression (1.15) shows that the displacement of air into the phasing plug x_t mitigates the compression (second and third right-hand terms). Since the displacement x_t is essentially the function of the chamber's pressure, it is fair to say that the stiffness of air in compression chamber is a function of diaphragm displacement and sound pressure in the chamber. Klippel performed derivation of chamber's compliance as a function of pressure and diaphragm's displacement in [4].

From the other hand the displacement of air particles x_t depends on the horn's impedance or in other words on the relationship between the sound pressure in the chamber and the particle velocity at the entrance of the phasing plug. The smaller the air displacement at the phasing plug entrance, the more pronounced are effects related to the nonlinear compression of the air in the chamber and higher is the pressure in the chamber. Alternatively, the higher the air displacement of air particles at the entrance of the phasing plug, the lower is nonlinear compression and lower is the pressure in the chamber. At low frequencies where the displacement of the diaphragm is maximum, the impedance of the acoustical load (phasing plug + horn) is low, the air is freely pulled in and pushed out of the chamber and the level of sound pressure is low. At higher frequencies, the chamber gets progressively "closed" by the acoustic load's impedance, and the sound pressure and the compression distortion increase. At high frequencies however, the velocity and displacement of the diaphragm diminish under the influence of moving mass and voice coil inductance. Furthermore the compliance of air in the compression chamber results in additional high-frequency roll-off. These factors cause the decrease of compression distortion at high frequencies.

Expression (1.14) for the compression chamber's pressure as a function of displacements x and x_t can be easily transformed into differential equation if we assume that the input impedance of the phasing plug and horn is $\rho_0 c$. This hypothesis is fair for the frequency range between the roll-off of the acoustical impedance at low frequencies and the advent of higher order modes within horn at high frequencies. Therefore, the displacement of air particles at the entrance of phasing plug can be approximated as follows:

$$x_t(t)=\int v_t(t)=\frac{1}{\rho_0 c}\int p(t)dt \quad (1.16)$$

where $v_t(t)$ is the velocity of air particles at the entrance of the phasing plug.

After substitution of (1.16) into (1.13) and corresponding manipulations to get rid of pressure integral, the nonlinear differential equation for the sound pressure in the chamber can be obtained:

$$\frac{dp}{dt}=\frac{\rho_0 c^2}{V_0}\left(\frac{p+P_0}{P_0}\right)^{\frac{1}{\gamma}+1}\left(S_{eff}\frac{dx}{dt}-\frac{S_t}{\rho_0 c}p\right) \quad (1.17)$$

The nonlinearity in equation (1.17) is caused by the term $\left[(p+P_0)P_0^{-1}\right]^{\frac{1}{\gamma}+1}$, which produces nonlinear distortion at high levels of sound pressure p comparable with atmospheric pressure P_0. At low levels of input signal the sound pressure in compression chamber satisfies condition $p << P_0$ and equation (1.17) takes the linear form:

$$\frac{dp}{dt}=\frac{\rho_0 c^2 S_{eff}}{V_0}\frac{dx}{dt}-\frac{cS_t}{V_0}p \quad (1.18)$$

Therefore, when the chamber is loaded by the phasing plug (and horn) the relationship between the displacement of the diaphragm and sound pressure becomes significantly more complex compared to that of the sealed chamber. This relationship is described by the nonlinear *differential* equation (rather than by a mere nonlinear equation) even when the loading acoustical impedance has a simplest $\rho_0 c$ form.

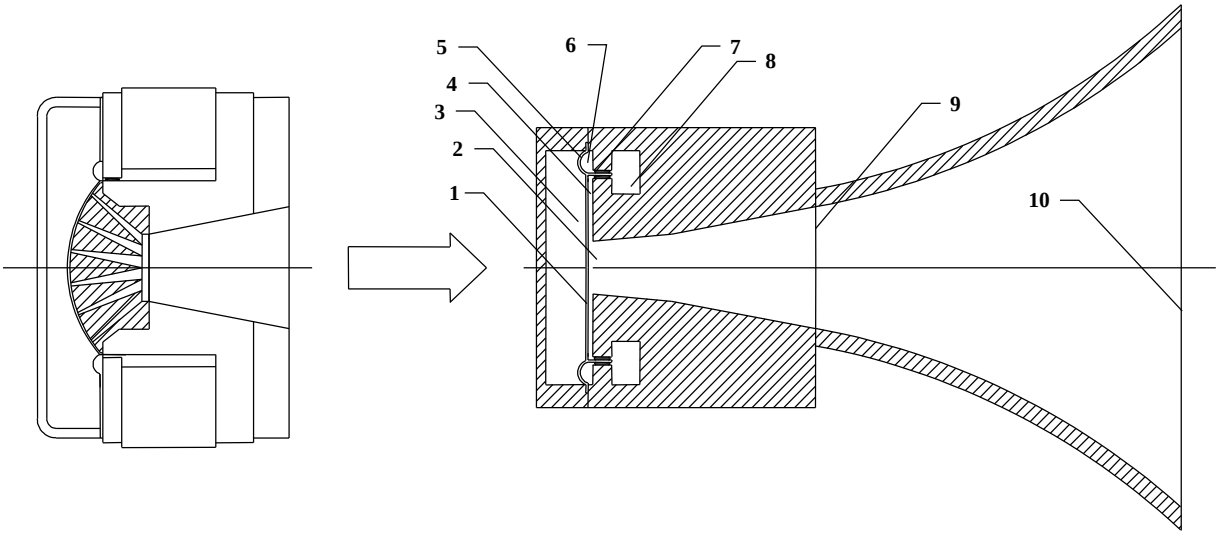

Fig. 1.3 Schematic diagram of compression driver used in experiments and modeling (a) and configuration of major mechanical and acoustical elements. 1. Diaphragm, 2. Phasing plug entrance, 3. Rear chamber, 4. Compression chamber, 5. Suspension, 6. Air cavity under suspension, 7. Voice coil in the gap with ferrofluid, 8. Air cavity behind the voice coil gap, 9. Output of phasing plug and throat of the horn, 10. Mouth of the horn.

Plane wave tube-loaded compression driver

To analyze the operation of compression driver, the expression for compression chamber's sound pressure (1.13) should be incorporated into a system of differential equations describing the movement of the diaphragm. Afterwards, the system of nonlinear differential equations can be solved numerically. However, there is a predicament to straightforward solution of this problem. The phasing plug and horn (see Fig. 1.3) acoustically load compression chamber. Therefore, the sound pressure in compression chamber depends on the impedance of this acoustical load. This impedance is a complex function of frequency and in general does not belong to the class of fractional-rational functions. This circumstance prevents direct transformation of horn's impedance (frequency domain) into a differential equation (time domain) to be included into the major system of differential equations describing compression driver's operation.

The seemingly possible alternative is calculating compression chamber's pressure by convolution of particle velocity at the entrance of acoustic load with the load's "impulse response". However, this approach does not work because it needs information about "future" velocity to convolve it with the impedance's impulse response. But this information is not known because the numerical solution of differential equations goes essentially one step at a time without "knowing" about the "remote future" of the particle velocity's behavior. In this sense numerical integration is myopic, whereas the convolution needs a "clear view" of the input signal over the duration of the pulse response of acoustic load.

To circumvent this problem, in this work the acoustical impedance of the horn was approximated by a fractional-rational function, and the latter was transformed into the system of differential equations relating the pressure and velocity at the entrance of the acoustical load (phasing plug + horn). The load's acoustical impedance is calculated numerically by the matrix method [8], [9], [10], [11]. Due to its flexibility the model of compression driver is potentially capable of taking into account the effects of force factor modulation (flux modulation) and the dependence of voice coil inductance on current, including hysteresis. The influence of eddy currents remains behind the scene in the derived equations to avoid cumbersome expressions. Actually it was taken into account by adding two extra components into the equation for the balance of voltages: eddy currents' losses R_2 and para-inductance L_2. The compression driver and horn used in experiments and modeling are shown in Fig. 1.4.

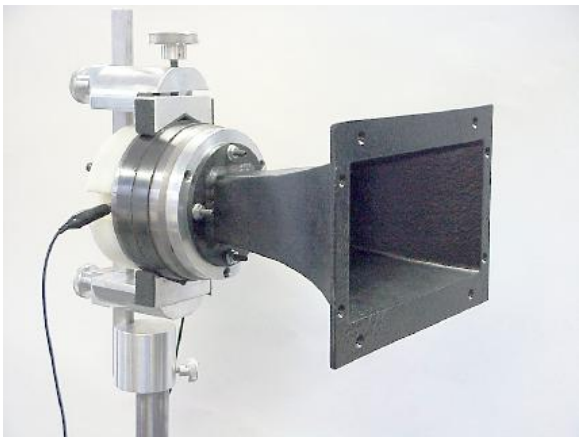

Fig. 1.4. Compression driver and horn used in measurements and modeling. Voice coil diameter 73 mm, driver exit 50 mm, length of the horn 210 mm.

Calculation of the compression chamber's air distortion is much simpler if a compression driver is loaded by the plane wave tube. In this case the problem with approximation of horn's impedance is obviated by replacing it with the constant impedance of the plane wave $\rho_0 c$. Strictly speaking, the modeling of the compression chamber's load by the "pure" $\rho_0 c$ is not completely accurate because the impedance of the phasing plug should be included into the modeling of the plane wave tube – loaded driver. However, for the purpose of clarity, the system of differential equations will be derived first for the case of "plane wave" loading, and then, the approximated impedance of the phasing plug and horn will be included in the model.

The system of equations describing operation of the compression driver whose chamber is $\rho_0 c$-loaded, takes the following form:

$$\begin{aligned} & m_{ms}\frac{d^2x}{dt^2}+\left[R_{ms}+R_{mv}(x)+R_t\left(\frac{dx_t}{dt}\right)\right]\frac{dx}{dt}+ \\ & +\left[K_{ms}(x)+K_{mr}(x)\right]x+\frac{1}{2}\frac{dL_{vc}(x,i_{vc})}{dx}i_{vc}^2+ \\ & +pS_{eff}=Bl(x,i_{vc})i_{vc} \end{aligned} \tag{1.19}$$

$$\begin{aligned} U = {} & R_{vc}i_{vc}+L_{vc}(x,i_{vc})\frac{di_{vc}}{dt}+ \\ & +\frac{dL_{vc}(x,i_{vc})}{dx}\frac{dx}{dt}+Bl(x,i_{vc})\frac{dx}{dt} \end{aligned} \tag{1.20}$$

$$P_0V_0^{\gamma}=(P_0+p)(V_0-V)^{\gamma} \tag{1.21}$$

$$V=S_{eff}x-S_tx_t \tag{1.22}$$

$$p=\rho_0 cv_t=\rho_0 c\frac{dx_t}{dt} \tag{1.23}$$

where m_{ms} is the diaphragm moving mass, R_{ms} is the suspension mechanical losses, R_{mv} is the thermoviscous losses in the compression chamber, R_t is the losses caused by turbulence in the phasing plug, K_{ms} is the suspension stiffness, K_{mr} is the rear chamber air stiffness, Bl is the force factor, p is the sound pressure in compression chamber, S_{eff} is diaphragm's effective area, L_{vc} is the voice coil inductance depending on voice coil current, in general including hysteresis.

Equations (1.19) and (1.20) resemble corresponding equations for the balance of forces and voltages in a low frequency loudspeaker with exception for the force term pS_{eff} responsible for the acoustic reaction of the compression chamber affecting diaphragm' movement. Equation (1.21) stands for the nonlinear dependence between the variation of the volume of the compression chamber and the pressure in it. Equation (1.22) accounts for the dynamic variation of chamber air's volume. Finally, equation (1.23) denotes boundary conditions at the entrance of the chamber's exit assuming plane-wave-loading impedance. It describes the relationship between the sound pressure in the chamber and particle velocity at the entrance of the phasing plug.

Nonlinear component of suspension's stiffness $K_{mr}(x)$ caused by adiabatic compression of air in the sealed rear chamber is calculated as:

$$K_{mr}(x)=S_{eff}^2P_0V_r^{\gamma}\gamma(V_r-S_{eff}x)^{-\gamma-1} \tag{1.24}$$

where V_r is the volume of the sealed rear chamber.

The mechanical losses term consists of three components, one of the them R_{ms} stands for the losses in mechanical parts of suspension, the second term, air flow resistance $R_{mv}(x)$, accounts for the thermoviscous losses in compression chamber [12],

and the third term $R_t\left(\frac{dx_t}{dt}\right)$ stands for the losses caused by the turbulence in the phasing plug.

To solve the system of equations (1.19) – (1.23), they are turned into the numerically integrable form:

$$\frac{di_{vc}}{dt} = \frac{1}{L_{vc}(x, i_{vc})}\left[U - R_{vc} i_{vc} - Bl(x, i_{vc})v\right] \quad (1.25)$$

$$\frac{dx}{dt} = v \quad (1.26)$$

$$\begin{aligned}\frac{dv}{dt} = \frac{1}{m_{ms}}\{&Bl(x, i_{vc}) i_{vc} - \\ &-\left[R_{ms} + R_{mv}(x) + R_t(v_t)\right]v - \\ &-\left[K_{ms}(x) + K_{mr}(x)\right]x - \\ &-\frac{1}{2}\frac{dL_{vc}(x, i_{vc})}{dx} i_{vc}^2 - p S_{eff}\Big\}\end{aligned} \quad (1.27)$$

$$\frac{dx_t}{dt} = v_t = \frac{p}{\rho c} \quad (1.28)$$

$$V = S_{eff} x - S_t x_t \quad (1.29)$$

$$p = P_0\left[\left(1 - V/V_0\right)^{-\gamma} - 1\right] \quad (1.30)$$

The system of equations (1.25) – (1.30) corresponds to the simplest form of the frequency-independent loading impedance $\rho_0 c$, which hardly exists in reality. Even with this simplification the solution of the problem is not trivial. The equations (1.25) – (1.30) have been derived for the explanatory purpose and clarity, and for a "smooth transition" to more sophisticated case of frequency-dependent acoustical loading impedance analyzed in the next paragraph.

Horn loaded compression driver

Derivation of the system of differential equations that takes into account acoustical load's impedance needs approximation of the impedance by a fractional-rational function:

$$\frac{1}{N}\sum_{n=1}^{N}\left[\left|Z_h(s_n)\right| - \left|Z_t(s_n)\right|\right]^2 \Rightarrow \min \quad (1.31)$$

$$s_n = i\omega_n,\ \omega_n \in \left\{\omega_{\min}, \omega_{\max}\right\}$$

where $Z_h(s)$ is the numerically calculated or measured complex impedance of the acoustical load (phasing plug + horn), $Z_t(s)$ is the approximating fractional-rational function:

$$Z_t(s) = \frac{p(s)}{v_t(s)} = \rho c \prod_{i=1}^{n} \frac{s^2 + b_{1i} s + b_{0i}}{s^2 + a_{1i} s + a_{0i}} \quad (1.32)$$

Particle velocity and displacement at the entrance of the phasing plug can be expressed as $v_t(s) = s x_t(s) = p(s)/Z_t(s)$. Combining for simplicity three terms of mechanical losses and two components of suspension stiffness into single parameters $R_m = R_{ms} + R_{mv} + R_t$ and $K_m = K_{ms} + K_{mr}$ and using inverse Laplace transform to turn acoustical impedance into differential operator, the system of equations taking into account load's complex acoustical impedance is compiled.

Particle displacement at the entrance of the phasing plug is expressed through the chamber's sound pressure and its derivatives. In general form:

$$\begin{aligned}\frac{d^n x_t}{dt^n} = \frac{1}{\rho c}\Bigg(&\frac{d^{n-1} p}{dt^{n-1}} + \frac{d^{n-2} p}{dt^{n-2}} g_{n-2} + \ldots \\ &+ \frac{dp}{dt} g_1 + p\, g_0\Bigg) - \frac{d^{n-1} x_t}{dt^{n-1}} h_{n-1} - \\ &- \frac{d^{n-2} x_t}{dt^{n-2}} h_{n-2} \ldots - \frac{dx_t}{dt} h_1\end{aligned} \quad (1.33)$$

After substitution of x_t and x into expression for the pressure (1.30) and its derivatives, the expression (1.33) is transformed into the following integrable form:

$$\frac{d^n x_t}{dt^n} = F\left[\frac{d^{n-1} x_t}{dt^{n-1}}, \cdots, x_t, \frac{d^{n-1} x}{dt^{n-1}}, \cdots, x\right] \quad (1.34)$$

By numerically integrating equation (1.34) *n*-times we obtain x_t:

$$\begin{cases} \dfrac{d^n x_t}{dt^n} \Rightarrow \dfrac{d^{n-1} x_t}{dt^{n-1}} \\ \cdots \\ \dfrac{dx_t}{dt} \Rightarrow x_t \end{cases} \tag{1.35}$$

Symbol $\Rightarrow$ denotes numerical integration performed by the Runge-Kutta algorithm. If, for example, the horn impedance is approximated by the function $Z_t(s) = \rho c s^2 / \left(s^2 + a_1 s + a_0\right)$, then, taking into account (1.33), equation (1.34) takes the form:

$$\frac{d^3 x_t}{dt^3} = \frac{1}{\rho c}\left(\frac{d^2 p}{dt^2} + a_1 \frac{dp}{dt} + a_0 p\right) \tag{1.36}$$

where a_1 and a_0 are the approximating coefficients.

After expressing the chamber's nonlinear sound pressure and its first and second derivative through x and x_t, equation (1.36) takes the following form:

$$\frac{d^3 x_t}{dt^3} = \Psi\left[\frac{d^2 x_t}{dt^2}, \frac{dx_t}{dt}, x_t, \frac{d^2 x}{dt^2}, \frac{dx}{dt}, x\right] \tag{1.37}$$

where $\Psi[\cdot]$ denotes nonlinear function of two displacements (of the diaphragm and of the air particles at the entrance of the phasing plug), and these displacements' first and second derivatives.

Applying numerical integration algorithm three times, displacement of air particles at the entrance of phasing plug is obtained:

$$\begin{cases} \dfrac{d^3 x_t}{dt^3} \Rightarrow \dfrac{d^2 x_t}{dt^2} \\ \dfrac{d^2 x_t}{dt^2} \Rightarrow \dfrac{dx_t}{dt} \\ \dfrac{dx_t}{dt} \Rightarrow x_t \end{cases} \tag{1.38}$$

Equations describing the voice coil displacement's second derivative (acceleration) is:

$$\begin{aligned} \frac{d^2 x}{dt^2} = \frac{1}{m_{ms}}\Bigg[& Bl(x, i_{vc}) \frac{di_{vc}}{dt} - \\ & - R_m(x) \frac{dx}{dt} - K_m(x) \frac{dx}{dt} - \\ & - \frac{i_{vc}^2}{2} \frac{dL_{vc}(x, i_{vc})}{dx} - pS_{eff} \Bigg] \end{aligned} \tag{1.39}$$

Integrating (1.39) twice, the displacement of diaphragm is obtained:

$$\begin{cases} \dfrac{d^2 x}{dt^2} \Rightarrow \dfrac{dx}{dt} \\ \dfrac{dx}{dt} \Rightarrow x \end{cases} \tag{1.40}$$

Expressions for the voice coil current's first derivatives is:

$$\begin{aligned} \frac{di_{vc}}{dt} = \frac{1}{L_{vc}(x, i_{vc})}\Big[& U - R_{vc} i_{vc} - \\ & - Bl(x, i_{vc}) \frac{dx}{dt} - i_{vc} \frac{dL_{vc}(x)}{dx} \frac{dx}{dt} \Big] \end{aligned} \tag{1.41}$$

Integration of (1.41) obtains voice coil current:

$$\frac{di_{vc}}{dt} \Rightarrow i_{vc} \tag{1.42}$$

Compression chamber's sound pressure *p* and its first and second derivatives $\frac{dp}{dt}$, $\frac{d^2 p}{dt^2}$ are calculated using analytical expressions obtained from (1.30) with equation (1.29) substituted in it. For example, chamber's sound pressure and its first two derivatives take the form:

$$p = P_0\left[V_0^{\gamma} V_d^{-\gamma}(x, x_t) - 1\right] \tag{1.43}$$

$$\frac{dp}{dt} = P_0 V_0^{\gamma} \gamma V_d^{-\gamma-1}(x, x_t) \Theta_1(x, x_t) \tag{1.44}$$

$$\frac{d^2 p}{dt^2} = P_0 V_0^{\gamma} \gamma \left[(\gamma+1) V_d^{-\gamma-2}(x, x_t) \Theta_1^2(x, x_t) - V_d^{\gamma-1}(x, x_t) \Theta_2(x, x_t) \right] \quad (1.45)$$

where

$$V_d(x, x_t) = \left(V_0 - S_{eff}\, x + S_t x_t \right) \quad (1.46)$$

$$\Theta_1(x, x_t) = \left(S_{eff} \frac{dx}{dt} - S_t \frac{dx_t}{dt} \right) \quad (1.47)$$

$$\Theta_2(x, x_t) = \left(S_{eff} \frac{d^2 x}{dt^2} - S_t \frac{d^2 x_t}{dt^2} \right) \quad (1.48)$$

The final result of numerical solution of the system of equations (1.33) – (1.48) is the nonlinear sound pressure in the compression chamber. Therefore, the influence of loading impedance on the complex nonlinear oscillation of the air in the compression chamber is taken into account. Afterwards, this pressure is used as an input signal for modeling of nonlinear propagation distortion in phasing plug and horn. This subject will be discussed further.

Other distortions in compression drivers

The distortions considered above are not unique in compression drivers. As mentioned, high frequency breakups of the diaphragm are another serious source of nonlinear distortion in compression drivers. Modeling of this phenomenon requires much more sophisticated approach. Mechanical nonlinear breakups are especially pronounced in metallic diaphragms, titanium being probably the worst case due to the specific "signature" of diaphragm's high frequency breakups. These breakups may produce one positive effect on performance of the compression driver. Due to the increased diaphragm displacement amplitude at partial high frequency resonances, the high frequency output increases. The price paid for the extended frequency range is nonlinear distortion that is generated at high frequencies, but affects lower frequency range of compression driver through difference intermodulation products.

The model developed here operates with lumped parameters. It means that the displacement of the diaphragm surface is assumed uniform, as is the distribution of sound pressure in the chamber. Taking into account a non-uniform distribution of chamber's nonlinear sound pressure and diaphragm's nonlinear distributed vibration is a much more intricate task that needs numerical solution of partial nonlinear differential equations with special boundary conditions. The problem is aggravated by the fact that the high frequency nonlinear oscillation of the chamber's air is coupled with the diaphragm's nonlinear breakups. The nonlinear coupling problem is difficult to model, especially if the reaction to a complex non-stationary signal is to be found. Thus far, the author does not know of any working engineering models and software based upon this level of sophistication.

Several other types of distortion may occur in a compression driver as well, such as the turbulent airflow in the phasing plug and voice coil gap. This mechanism may start "working" at very high levels of signal when the amplitude of particle velocity exceeds Reynolds number. This effect causes abrupt increase in the airflow resistance. Accurate modeling of turbulent airflow also needs a solution of nonlinear partial differential equations. In this work the modeling of distortion caused by the advent of turbulence in the phasing plug was theoretically considered by the mechanical resistance dependent on velocity of airflow in the phasing plug. Practically, this approach needs information about dependence of acoustical losses on airflow velocity in the phasing plug. This approach seems viable but needs further elaboration. Therefore, the term $R_t(v_t)$ presented in the modeling equations has not been currently "turned on". Increase of the voice coil temperature and resistance at high levels of input signal may be considered as another source of sound quality deterioration due the change of the frequency response and dynamic compression of output SPL.

Table 1

Bl	**K_{ms}**	**K_{mr}**	**m_{ms}**	**R_{ms}**	**R_{mv}**	**R_{vc}**	**R_2**	**L_1**	**L_2**	**S_{eff}**	**S_t**	**V_0**	**h**	**V_r**
Tm	N/ mm	N/ mm	g	kg/s	kg/s	Ohm	Ohm	mH	mH	cm^2	cm^2	cm^3	mm	cm^3
21.2	40.4	24.5	5.22	3.9	3.9	10.2	9.3	0.84	0.66	47.3	3.8	4.7	1.0	129

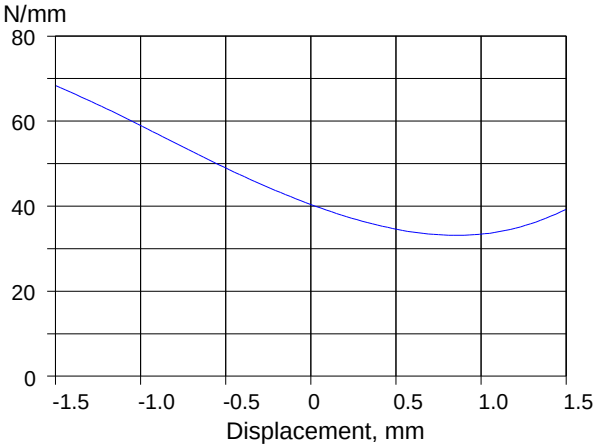

Fig. 1.5a. Suspension stuffiness $K_{ms}(x)+K_{mr}(x)$ of compression driver as a function of voice coil displacement.

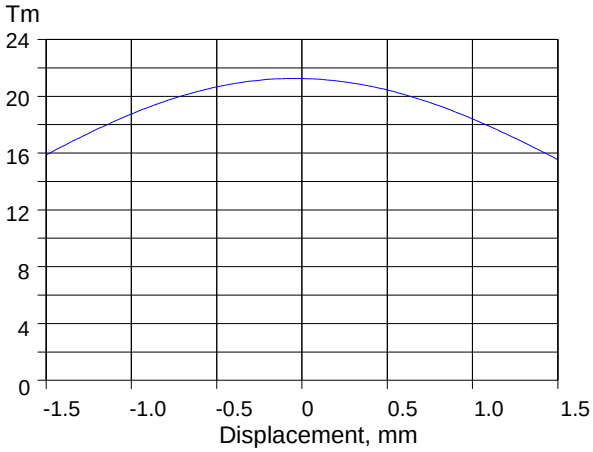

Fig. 1.5c. Bl-product $Bl(x)$ of compression driver as a function of voice coil displacement.

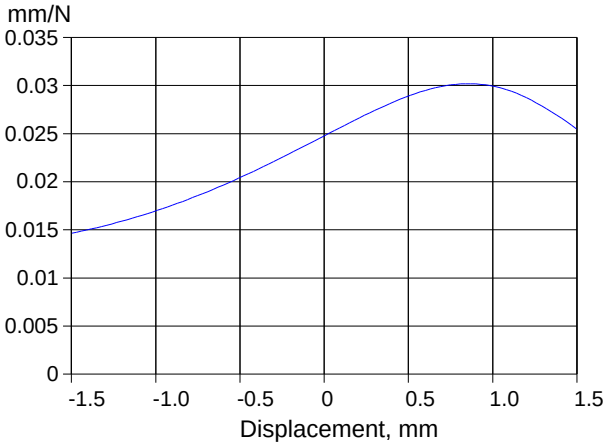

Fig. 1.5b. Suspension compliance $C_{ms}(x)$ of compression driver as a function of voice coil displacement.

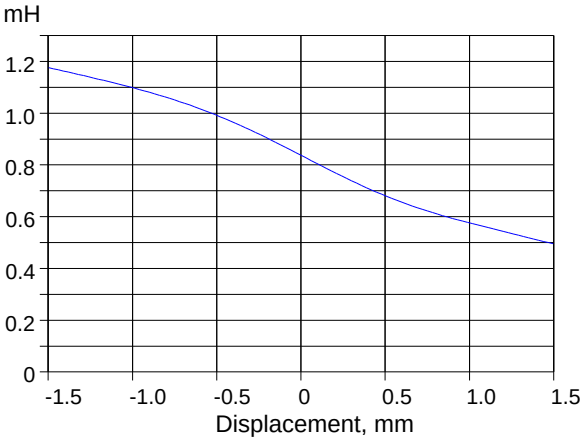

Fig. 1.5d. Voice coil inductance $L_{vc}(x)$ of compression driver as a function of voice coil displacement.

Fig. 1.5 shows the excursion-dependent parameters of compression driver measured by the Klippel Analyzer. Similarly to the approach used in [12], the steady state value of airflow resistor responsible for modulation of thermoviscous losses was chosen $R_{mv}(x_0) = R_{ms}$. Two different dependencies of $R_{mv}(x)$ on excursion were simulated: one of them assumes $R_{mv}(x)$ proportional to $1/h(x)$, the other assumes $R_{mv}(x)$ proportional to $1/h^2(x)$ where $h(x)$ is the effective height of the compression chamber. The former dependence approximates high frequency flow resistance, whereas the latter describes low frequency flow resistance [12]. This is an approximate approach, accurate modeling of this effect needs much more involved methods based on solution of nonlinear partial differential equations taking into account thermoviscous losses and complex boundary conditions depending on the compression chamber's geometry and loading.

In this example the impedance of the horn was approximated by the fractional-rational function of the second order. This approximation puts the particle displacement at the entrance of phasing plug and sound pressure in compression chamber into the relationship:

$$\frac{d^3 x_t}{dt^3} = \frac{d^2 p}{dt^2}\frac{1}{\rho c} + \frac{dp}{dt}\frac{a_0}{\rho c} + p\frac{a_1}{\rho c}. \qquad \text{Phasing}$$

plug and horn were considered as a single acoustical load with approximately exponential flare. The length of the equivalent horn is 305 mm, equivalent mouth diameter is 200 mm, equivalent throat diameter is 22 mm. Fig. 1.6 shows the modulus of impedance of the horn modeled numerically through the use of matrix method [10], and the modulus of approximating function. Fig. 1.7 shows the modeled SPL (fundamental) in the chamber. The SPL measured and modeled at the mouth of the horn will be shown in the next section and analyzed in more detail when the performance of the horn will be discussed. Fig. 1.8 illustrates separate influence of different nonlinear effects on THD. The level of input voltage 12 V RMS provides 120 dB RMS SPL at 1 meter from the horn's mouth. Fig. 1.9 shows the effect of increase of the signal on the overall THD in compression chamber taking into account all considered nonlinear effects.

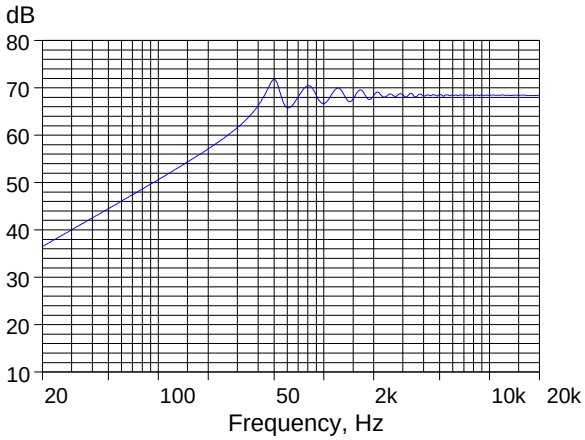

Fig. 1.6a. Modulus of acoustic load impedance (phasing plug + horn). Numerically calculated through the use of matrix analysis

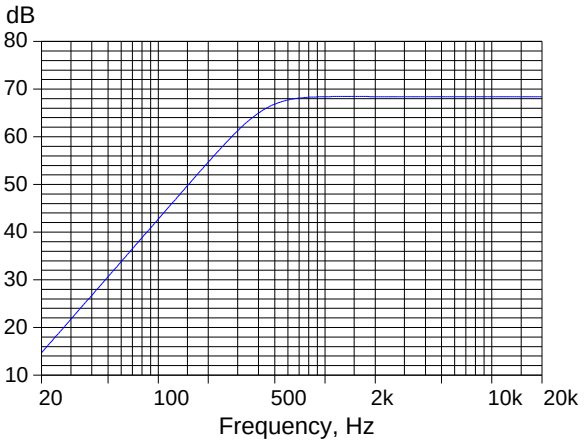

Fig. 1.6b. Modulus of acoustic load impedance (phasing plug + horn). Approximated by the second order fractional-rational function to transform impedance into differential operator.

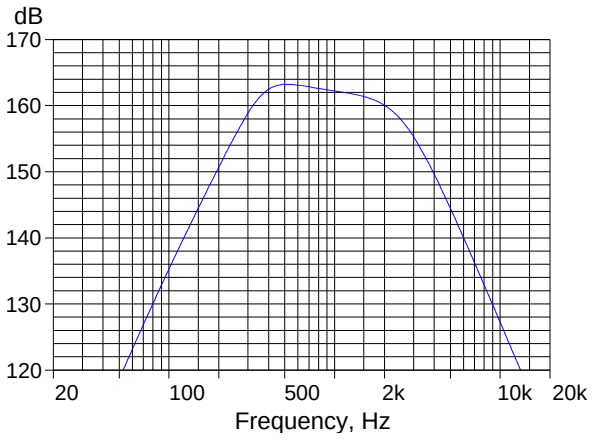

Fig. 1.7. Fundamental of SPL in compression chamber

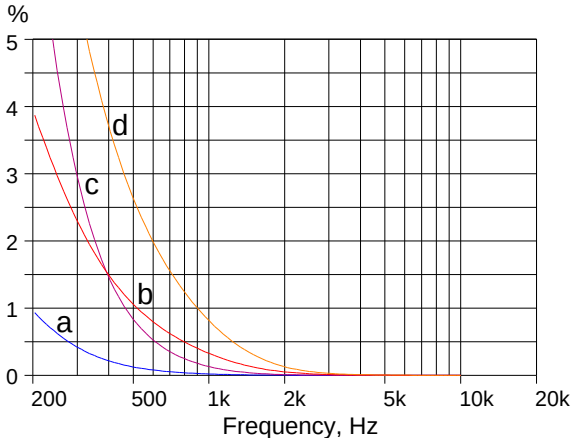

Fig. 1.8a. THD in compression chamber produced by different nonlinear mechanisms. a – rear chamber stiffness, b – chamber airflow (1st order), c – suspension stiffness, d – chamber airflow (2nd order).

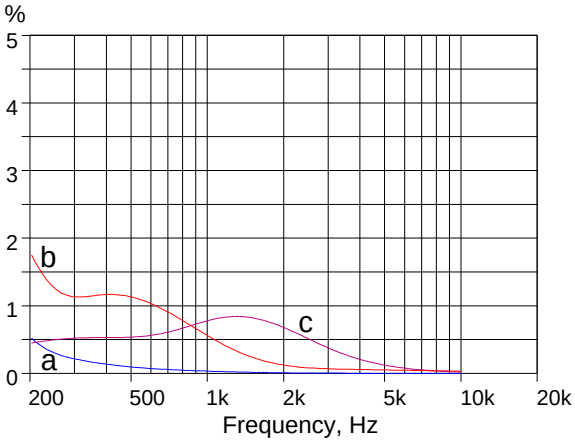

Fig. 1.8b. THD in compression chamber produced by different nonlinear mechanisms. a – Bl-product, b – inductance modulation, c – nonlinear air compression.

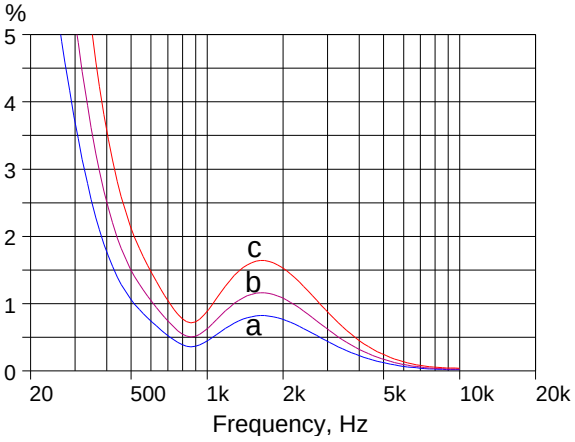

Fig 1.9. Compression chamber sound pressure. THD produced by all nonlinear sources. a – Input voltage 12 V RMS, b – input voltage increased by 3 dB, c – input voltage increased by 6 dB.

The results of the modeling show that at "low" frequencies the THD produced by nonlinear mechanisms related to excursion-dependent parameters prevail. These parameters are the Bl-product, mechanical stiffness of suspension, nonlinear stiffness of air in the rear chamber, and nonlinear airflow in compression chamber. At high frequencies the distortion produced by the nonlinear adiabatic compression of air in the front chamber and the distortion produced by the voice coil inductance variation dominates. The distortion produced by the air nonlinearity is maximum at mid frequencies around 1 kHz – 2 kHz. This distortion depends on the degree of air compression i.e. on the relative change of the air chamber's volume. If the chamber were closed at all, this distortion would be huge reaching its peak at the maximum of diaphragm displacement. The larger the area of the phasing plug's entrance, the less is the "closing" effect produced by the impedance of the phasing plug and horn. Therefore, the less is compression and nonlinear distortion. With the decrease of compression, the efficiency of compression driver goes down as well. So, the design of compression driver is always a compromise between the efficiency and nonlinear distortion. Theoretically the maximum efficiency of horn driver (50 %) is never reached in practical designs because of the various electromechanical and mechanical losses of energy (eddy currents, hysteresis in motor, losses in suspension, etc.). In addition, the maximum efficiency conditions may not correspond to the maximum flatness and width of horn driver's frequency response.

The modeling shows that at the particular level of input signal (12 V RMS amplitude that maintains 120-dB half-space RMS SPL at 1 meter from the horn) the share of the air compression distortion is not desperately high. However, the level of sound pressure in the chamber, that reaches 165 dB SPL, is very critical for generation of propagation distortion in phasing plug and horn. At this level of signal, distortion produced by nonlinear air compression may not be a serious problem, reaching modest (for sound reinforcement equipment) 0.85 % at 1.5 kHz. However, this level of compression distortion is indicative of the high SPL in the chamber that will cause propagation distortion in sound waves traveling through the phasing plug, horn, and further in free air. At higher levels of input signal the air distortion in compression chamber increases further, that presents a problem in its own right even if driver were used without a phasing plug and the horn. But this high level of pressure at the entrance of the phasing plug

produces truly devastating effect on sound quality reincarnating in the form of harmful air propagation distortion at the mouth of the horn, and further at the listener's ears.

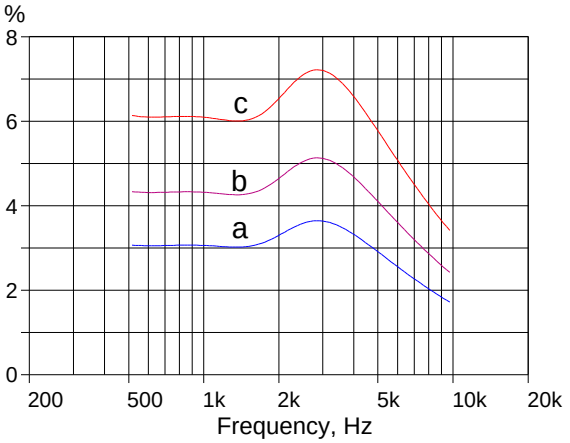

Fig. 1.10. Compression chamber sound pressure. TTIMD produced by all nonlinear sources. a – Input voltage 12 V RMS, b – input voltage increased by 3 dB, c – input voltage increased by 6 dB.

Fig. 1.10 shows the two-tone total intermodulation distortion (TTIMD) distortion produced by all nonlinear effects. The increase of TTIMD between 2 kHz and 3 kHz reveals modulation of the swept high frequency signal by the fixed low frequency (500 Hz) tone. The TTIMD was calculated as:

$$d_{TTIMD} = \frac{\sqrt{\sum_{i=1}^{N} p_i^2}}{P_f} \times 100\,\% \qquad (1.49)$$

where $p_1 = P_{f_2+f_1}$, $p_2 = P_{f_2-f_1}$, $p_3 = P_{2f_2+f_1}$, $p_4 = P_{2f_2-f_1}$, $p_5 = P_{f_2+2f_1}$, $p_6 = P_{f_2-2f_1}$, $p_7 = P_{3f_2+f_1}$, $p_8 = P_{3f_2-f_1}$,….. are the amplitudes of the intermodulation products, $P_f = P_{f_1} = P_{f_2}$ is the amplitude of either one of fundamental tones, f_1 is the fixed low frequency tone , f_2 is the higher frequency sweeping tone. The products up to the tenth order were included in calculation of TTIMD in current work.

In this approach the excitation signal consists of two tones having equal amplitudes. One of these two tones is swept across the frequency range. The level of TTIMD, calculated according to (1.49), is plotted at the frequency of the sweeping tone. This method to calculate TTIMD takes into account higher order nonlinearity, but not completely, because it does not include all possible IM products excited by the two-tone signal such as other products of the kind $P_{nf_2 \pm mf_1}$, $n \neq m \neq 1$.

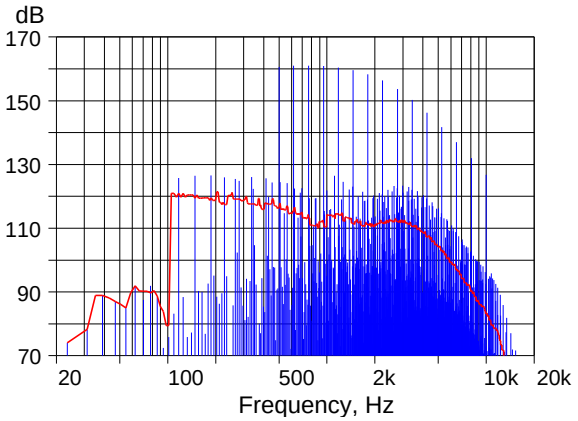

Fig. 1.11. Sound pressure in compression chamber. Reaction to multitone stimulus.
Sold curve – multitone total nonlinear distortion.

Fig. 1.11 illustrates reaction of compression chamber's pressure to multitone stimulus with all nonlinear mechanisms accounted. This is the most informative criterion of nonlinearity assessment among those used in this work. Reaction to multitone stimulus includes variety of intermodulation components and is capable to reveal nonlinear effects not observed through the use of swept sinusoidal tones. For example, the graph on Fig. 1.11 shows that the difference-frequency intermodulation components are generated not only within the frequency range of testing signal, but well below it. It means that no matter how steep is a high-pass filter used with this compression driver, nonlinear products will be inevitably generated and radiated below the filter's cut-off frequency. A real compression driver exhibits higher level of distortion than a model. The difference is attributed to the nonlinear breakups of the diaphragm and other nonlinear effects not taken into account, such as flux modulation, magnetic hysteresis and possibly non-laminar airflow in the phasing plug. The role of each of these effects played in performance of a compression driver needs further, more detailed investigation and analysis.

The reaction to multitone stimulus depicted on Fig. 1.11 is overlaid with the curve of frequency-dependent multitone total nonlinear distortion

coefficient (MTND). This nonlinear characteristic is an integral criterion that makes it possible to express the reaction to multitone in the form of the single frequency-dependent curve which is easy to be "grasped" visually, and could be expressed in percent against fundamental or overlaid with other curves obtained at different levels of input signal or corresponding to different devices under test (DUT). The crux of MTND is to show the energy of distortion products averaged in certain frequency bands. There are various ways to do it, such as for example, plotting the average level of distortion products in 1/3-octave bands. Then MTND looks as a bar diagram. In this work distortion products (harmonic and intermodulation) are averaged within a 1/3 octave-wide rectangular sliding window. The averaged sum of distortion products is plotted at the mid-frequency of the window, then the widow is slided one frequency bin up and the new averaged value of distortion products is calculated. The frequency samples corresponding to primary tones are omitted. Hence, the continuous frequency response of multitone total nonlinear distortion (MTND) is obtained and plotted.

$$d_{MTND}(f_i) = \sqrt{\frac{1}{K}\sum_{k=1}^{K} D_k^2} \qquad (1.50)$$

where D_k is a distortion product (either harmonic or intermodulation) at the frequency f_k, the current frequency f_i corresponds to the midpoint of the sweeping rectangular window 1/3 octave wide. The window consists of K samples.

This method helps to obtain a simple graphical interpretation of nonlinear reaction to multitone and makes it possible to easily plot reaction to various levels of input signal. The viability of this way to plot reaction to multitone is yet to be determined, including correlation with distortion audibility.

HORN

The primary goal of a horn is to provide certain SPL coverage, the constant directivity of a horn is usually the desirable goal. An important property of a horn is also the coupling of the high output mechanical impedance of the compression driver with the low impedance of the medium. Transmission of sound energy through a horn is associated with nonlinear distortion. Horns with slower flares are characterized by the larger nonlinear distortion. This distortion is an inevitable evil, inherent to practically all mid and high frequency horns. A reasonably accurate dynamic model of a horn may not only provide information about distortion at the mouth of a particular horn, but it may help in auralization of this distortion without building the horn. One-dimensional nonlinear model of a horn of arbitrary flare and length was developed in this work.

Similarly to the conceptual approach to modeling of woofers and compression drivers, the methods based on simple tonal signals and calculation of the nonlinear response in terms of harmonic distortion only were not considered [6]. Instead, the method based on modified matrix analysis of horns was employed. Matrix method is used in linear analysis of horns, and proved to be a convenient and flexible engineering tool [9], [10], [11]. Matrix method can be modified to model nonlinear distortion in horn, by splitting each modeling element into two sub-elements, each one of them consisting of linear and nonlinear part [8], [11]. This model works with periodic signals, including multitone with the bin-attached frequency components. Each linear section is described by the matrix of A-parameters and the calculation of the spectra of a sound wave at the outlet of each section is carried out merely by the multiplication of the spectrum of the signal at the inlet of the section with its transfer function, taking into account the loading impedance of the consequent section. Therefore, the modeling begins with the "backward" calculation of impedances at the input of each section. Furthermore, after calculation of the spectrum of the signal at the outlet of a current linear conical section, the spectrum is turned into the time domain through the use of inverse Fourier transform, and the time domain waveform is "put through" the nonlinear section, characterized by the nonlinear transformation of a plane sound wave. Therefore, such a model, that belongs to the class of Hammerstein-Wiener nonlinear models, ("sandwich" consisting of linear dynamic and nonlinear static subsystems [7]), describes one-dimensional propagation of a sound wave inside the horn, taking into account reflection of linear components from the mouth, and progressive nonlinear deterioration of sound wave on its way from the throat to the mouth.

In the model used earlier [11], the cylindrical sections were used to simulate linear distortion in the horn. It was decided later to use conical element instead. The model based on conical elements uses much less elements while providing similar accuracy.

Furthermore, the model was further developed to handle not only a periodic signal but the signal of arbitrary time dependence, such as musical signals. This was achieved through replacement of multiplication of the signal spectra with the transfer functions of cylindrical sections by the convolution of the signal with the pulse response of each conical section. The pulse responses were calculated trough the use of inverse Fourier transforms. This approach makes it possible to perform auralization of horn nonlinear distortion. Both methods will be considered in more detail.

Horn's nonlinear model for periodic signals

The model assumes that the reflections from the horn's mouth affect the signal in linear approximation, whereas the nonlinear products propagate without reflections. This assumption is fair for the frequency range above the horn's cut-off frequency, where horns are generally used. The block-diagram of the signal transformation is depicted on Fig. 2.1. Calculation in the frequency domain is carried out as follows: The complex particle velocity v_{ti} and pressure p_{ti} at the inlet of an *i*-th conical element and the particle velocity v_{mi} and pressure p_{mi} at the outlet are related by the following matrix equation:

$$\begin{bmatrix} p_{ti} \\ v_{ti} S_i \end{bmatrix} = [\mathbf{a_i}] \begin{bmatrix} p_{mi} \\ v_{mi} S_i \end{bmatrix} \tag{2.1}$$

where S_i is the spherical area of the inlet of the *i*-th conical element.

The matrix $[\mathbf{a_i}]$ is expressed through the geometrical parameters of the conical element as:

$$[\mathbf{a_i}] = \begin{bmatrix} a_{11i} & a_{12i} \\ a_{21i} & a_{22i} \end{bmatrix} \tag{2.2}$$

$$a_{11i} = \left(\frac{x_{1i}}{x_{0i}}\right)\cos(kl_i) - \left(\frac{1}{kx_{0i}}\right)\sin(kl_i) \tag{2.3}$$

$$a_{12i} = \left(\frac{x_{0i}}{x_{1i}}\right) jR_{0i}\sin(kl_i) \tag{2.4}$$

$$a_{21i} = \left(\frac{j}{R_{0i}}\right)\left[\left(\frac{x_1}{x_{0i}} + \frac{1}{(kx_{0i})^2}\right)\sin(kl_i) - \left(\frac{l_i}{x_{0i}}\right)\left(\frac{1}{kx_{0i}}\right)\cos(kl_i)\right] \tag{2.5}$$

$$a_{22i} = \left(\frac{x_{0i}}{x_{1i}}\right)\left[\cos(kl_i) + \left(\frac{1}{kx_{0i}}\right)\sin(kl_i)\right] \tag{2.6}$$

where $R_{oi} = \dfrac{\rho\, c}{S_i}$ is the normalized plane wave impedance, $k = \dfrac{\omega}{c}$ is the wave number, $j = \sqrt{-1}$, $x_{1i} = l_i + x_{0i}$ is the length of the cone's side from the base to the apex, l_i is the length of the side of the frustum, x_0 is the length of the side from the apex to the smaller base of the frustum.

The pressure at the outlet of the *i*-th element is related to the pressure at its inlet as:

$$p_{mi}(i\omega) = p_{ti}(i\omega)T_i(i\omega) \tag{2.7}$$

where $T_i(i\omega)$ is the transfer function of the *i*-th conical element loaded by $Z_{ami}(i\omega)$:

$$T_i(i\omega) = \frac{1}{a_{11i}(i\omega) + a_{12i}(i\omega)/Z_{ami}(i\omega)} \tag{2.8}$$

Z_{ami} is the complex loading impedance of the *i*-th conical element, which is in fact the input acoustical impedance of the next conical element $Z_{at(i+1)}$.

The input impedance of the (*i*+1)-th conical element is calculated as:

$$Z_{at(i+1)} = \frac{a_{11(i+1)}Z_{am(i+1)} + a_{12(i+1)}}{a_{21(i+1)}Z_{am(i+1)} + a_{22(i+1)}} \tag{2.9}$$

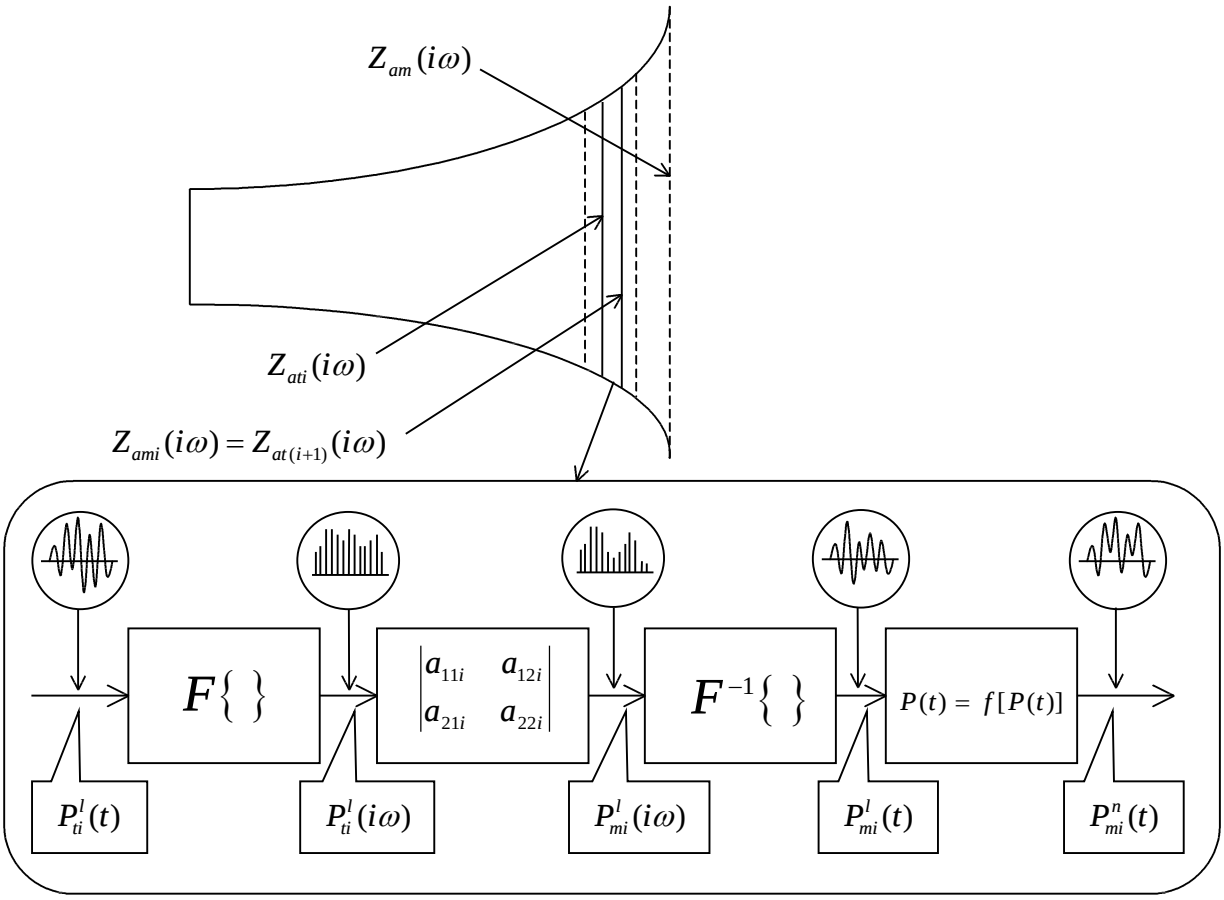

Fig. 2.1a. Schematic diagram of horn's modeling. Nonlinear model for periodic sound waves.

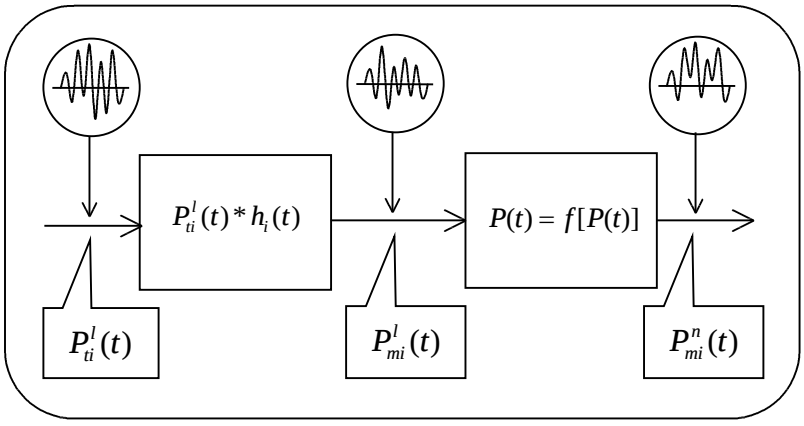

Fig. 2.1b. Schematic diagram of horn's modeling. Nonlinear model for non-periodic sound waves.

Calculation of sound pressure is preceded by the calculation of the 'throat" impedance of each conical element. This calculation begins from the input impedance of the last *n*-th conical element adjacent to the mouth of the horn. The inlet impedance of the last *n*-th element is calculated using expression for the radiation impedance of a piston:

$$Z_{amn} = \frac{\rho c}{S_m}\left[\left(1 - \frac{J_1(2kr_m)}{kr_m}\right) + i\frac{S_1(2kr_m)}{kr_m}\right] \quad (2.10)$$

where S_m is the mouth area, r_m is the mouth radius, $J_1(2kr_m)$ and $S_1(kr_m)$ are the first-order Bessel and Strouve functions, $i = \sqrt{-1}$.

The initial "linear" sound pressure $p_{t1}^l(i\omega)$ at the throat of the horn is obtained from the modeling of compression driver. It may as well be obtained from the measurement of the pressure at the output of compression driver. The pressure $p_{m1}^l(i\omega)$ at the outlet of the first linear element is calculated by (2.7): $p_{t1}^l(i\omega) \Rightarrow p_{m1}^l(i\omega)$. Then, using inverse Fourier transform, the spectrum of sound wave is transformed into the time domain: $p_{m1}^l(t) = F^{-1}\left\{p_{m1}^l(i\omega)\right\}$. The nonlinear response $p_{m1}^n(t)$ is found through the numerical solution of the implicit equation:

$$F\left[\tau + \frac{r}{c}\frac{\beta\, p_{m1}^n(\tau)}{(c + \beta\, p_{m1}^n(\tau))}\right] - p_{m1}^n(\tau) = 0 \quad (2.11)$$

where the time domain function $F[\cdot]$ denotes the waveform $p_{m1}^l(t)$, *c* is undisturbed sound speed, r is the distance from sound speed, $\beta = (\gamma + 1)/2$ is the nonlinearity coefficient, $\gamma = 1.4$, $\tau = t - r/c$ is retarded time.

Then, after transformation $p_{m1}^n(\tau) \Rightarrow p_{m1}^n(t)$, the pressure at the outlet of the first element is turned into the frequency domain and this spectrum is considered as an "input" for the next element see Fig. 2.1. This algorithm is continued until the spectrum of the pressure at the mouth is calculated. The chain of sound wave transformations in a single *i*-th element (consisting of a linear "dynamic" conical sub-element and nonlinear "static" cylindrical sub-element) looks as:

1. $p_{ti}^l(i\omega) \Rightarrow p_{mi}^l(i\omega)$ (linear transformation, output frequency response)
2. $p_{mi}^l(i\omega) \Rightarrow p_{mi}^l(t)$ (linear transformation, new output waveform)
3. $p_{mi}^l(t) \Rightarrow p_{mi}^l(\tau)$ (linear transformation into new time domain scale)
4. $p_{mi}^l(\tau) \Rightarrow p_{mi}^n(\tau)$ (nonlinear transformation, new "output" distorted waveform)
5. $p_{mi}^n(\tau) \Rightarrow p_{mi}^n(t)$ (linear transformation into real time scale)
6. $p_{mi}^n(t) \Rightarrow p_{mi}^n(i\omega)$ (linear transformation, new spectrum of distorted sound wave)
7. $p_{mi}^n(i\omega) \Rightarrow p_{t(i+1)}^l(i\omega)$ (step to the next element)

Horn's nonlinear model for non-periodic signals

In the previous model the linear transformation of the spectra was based on using matrix method and the implicit equation (2.11) to calculate the pressure at the output of an *i*-th element. This method is applicable only for periodic signals, including multitone whose frequency components are attached to frequency bins. However, this approach does not work if the reaction to a non-stationary signal is to be found. In this case multiplication of spectra does not work and the convolution of the input signal with the pulse response of the conical element should be used.

$$p_{mi}^l(t) = p_{ti}^l(t) * h_i(t) \quad (2.12)$$

Symbol * denotes convolution. To perform convolution, the linear transfer function of each conical element is turned into the corresponding pulse response:

$$h_i(t) = F^{-1}\left\{T_i(i\omega)\right\} \quad (2.13)$$

Afterwards, the "linear" pressure of the *i*-th element is transformed nonlinearly similar to the "periodic" model. The nonlinearly distorted pressure $p_{mi}^n(t)$ is calculated using (2.11). Then, the simulation goes to the next conical element. The pressure $p_{mi}^n(t)$ is considered an input signal for the next element: $p_{t(i+1)}^n(t) = p_{mi}^n(t)$. New transfer function

$T_{i+1}(i\omega)$ and new impulse response $h_{i+1}(t)$ are calculated according to (2.8) and (2.13) and then the expression (2.11) is used again to calculate further distorted pressure $p^{n}_{m(i+1)}(t)$. The calculation is continued until the pressure at the horn's mouth is found.

Modeling distortion in horn

The model developed was used to simulate distortion in the exponential horn 305 mm long, having 22-mm throat diameter and 200-mm equivalent diameter of the mouth (see Fig. 1.4). The phasing plug was considered the beginning of the horn. The pressure at the throat of the horn was taken from the calculation of the pressure at the output of the compression driver in the previous section. Fig. 2.2 shows modeled SPL of fundamental at the mouth of the horn. The input signal was generated by the model of the compression driver. The level of input voltage was set to 12 V RMS to provide 120 dB SPL at 1 meter from the horn's mouth to compare overall distortion in horn driver with distortion in woofer. Fig. 2.3 shows for comparison the SPL measured at the mouth of the real horn loaded by compression driver (see Fig. 1.4). Good agreement between modeled and measured characteristics is observed. The results of nonlinear modeling are shown in Fig. 2.4 and Fig. 2.5 where the THD and multitone distortion at the mouth of the horn are observed. The level of distortion produced by the horn (in combination with a phasing plug) at high frequencies is higher than the distortion produced by the compression driver. Fig. 2.6 shows for comparison distortion measured at the mouth of the horn. The level of measured distortion is higher than the model that can be explained by the influence of nonlinear mechanisms not taken into account in modeling of compression driver. These mechanisms are the nonlinear high frequency breakups of the diaphragm, flux modulation, magnetic hysteresis, and possibly, non-laminar airflow in the phasing plug.

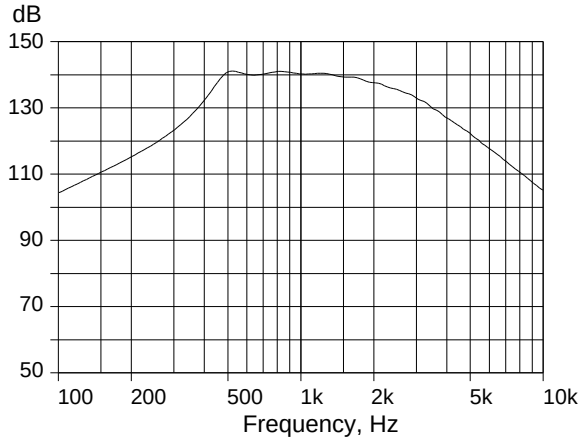

Fig. 2.2 Modeled SPL of fundamental at the mouth of the horn Input voltage at the compression chamber 12 V.

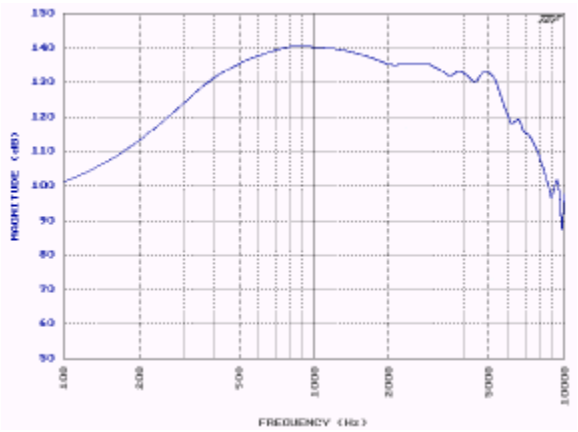

Fig. 2.3. Measured SPL of fundamental at the mouth of the horn Input voltage at the compression chamber 12 V.

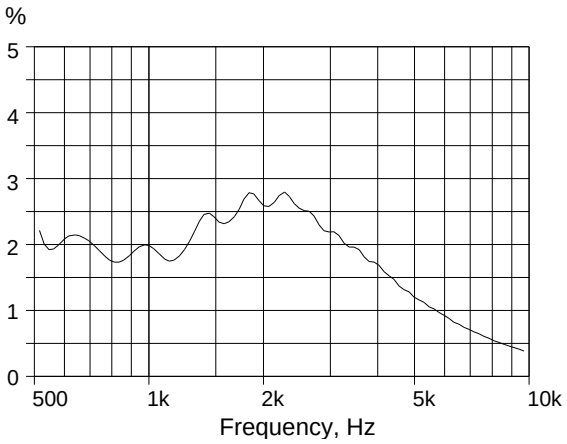

Fig. 2.4. Modeled SPL THD at the mouth of the horn. Input voltage at compression driver terminals is 12 V.

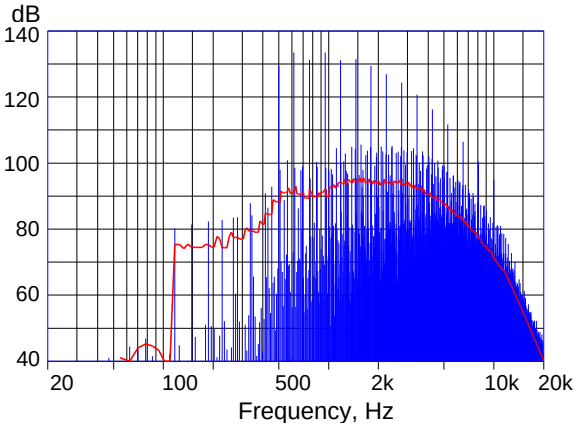

Fig. 2.5. Modeled multitone response at the mouth of the horn. Input voltage at compression driver terminals is 12 V. Sold curve – multitone total nonlinear distortion.

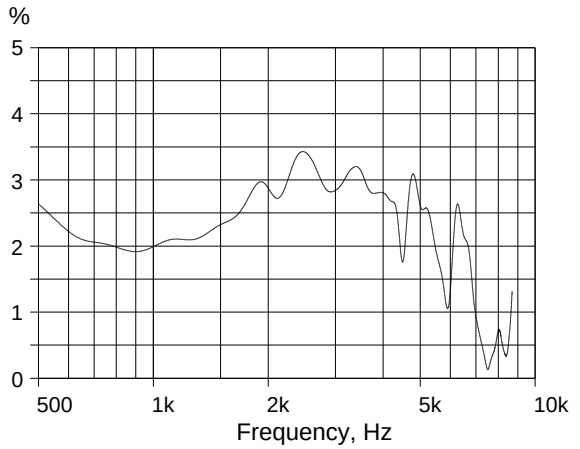

Fig. 2.6. Measured SPL THD at the mouth of the horn. Input voltage at compression driver terminals is 12 V.

As mentioned in the first section, the free air propagation distortion may be as significant as the distortion of a horn driver or even exceed it. A simple method to evaluate approximately the level of propagation distortion is the use of implicit equations describing propagation of one-dimensional waves (plane, cylindrical, and spherical). Expression (2.14) correspond to the propagation of spherical wave, the most "benign" of one-dimensional waves from the standpoint of propagation distortion:

$$v(\tau)-\frac{r}{r_0}F\left[\tau+\right.$$
$$\left.+\frac{\beta}{c_0^2}r_0\ln\left(\frac{r}{r_0}\right)\frac{r}{r_0}v(\tau)\right]=0 \qquad (2.14)$$

$\tau\in\{0,...\tau_m\}$

where $F[\cdot]$ is arbitrary function (band-limited noise, musical signal), $v(\tau)$ is particle velocity, r is the distance from he source, r_0 is the radius of the source, $\tau=t-r/c_0$ is retarded time, c_0 is the undisturbed sound speed, $\beta=(\gamma+1)/2$ is the coefficient of nonlinearity, with γ being the ratio of specific heat at constant volume to that at constant volume and having a value of 1.4 for air, $\{0,...\tau_m\}$ is the time interval where the solution is searched.

For each moment of time τ_i solution of equation (2.14) is searched numerically by the method of bracketing and bisection [13]. The solution is a value of particle velocity $v(\tau_i)$ corresponding to time τ_i and distance r. To calculate distortion in the pressure of a periodic sound wave, the spectrum of the distorted velocity is multiplied by the spectrum of the spherical wave impedance. Sound pressure of non-periodic waves is found through the convolution of velocity with inverse Fourier transform of spherical wave's impedance.

Fig. 2.7 shows THD of spherical wave at 1 meter from the source. The pressure at the source is equal to the pressure at the mouth of the horn 140 dB SPL. Fig. 2.8 shows the multitone distortion of this spherical wave. Fig. 2.9 shows THD measured at the same SPL at the mouth and the same distance from the mouth.

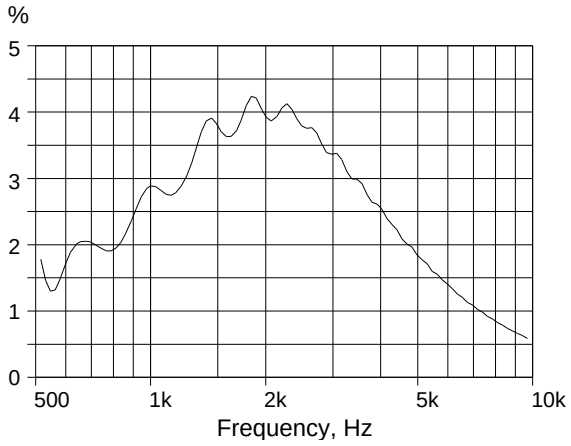

Fig. 2.7. Compression driver. THD modeled at 1 meter from the mouth. Spherical wave approximation.

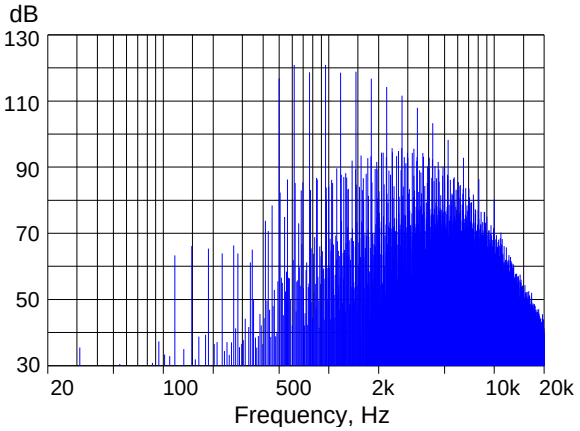

Fig. 2.8. SPL at 1 meter from the mouth of the horn.

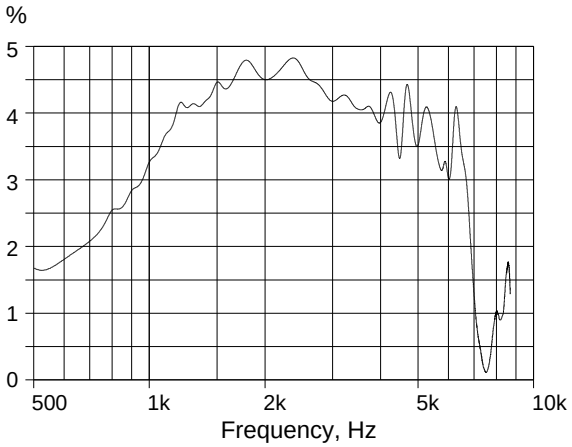

Fig. 2.9. Compression driver. THD measured at 1 meter from the mouth.

The modeling and measurement show that the level of propagation distortion is quite comparable with the distortion generated in the horn driver.

CONCLUSION

Accurate modeling of nonlinear distortion in a compression driver and horn is a step towards building an efficient and flexible design system. Such a system, if built, should minimize prototyping time, and help to determine the relative importance of various nonlinear mechanisms. This information would help to estimate what levels of nonlinear distortions are critical from their audibility standpoint. Such thresholds might provide valuable information that can be possibly used in the standards for loudspeaker objective parameters. This problem is general, it has not been solved thus far.

Accurate prediction of nonlinear distortion helps to avoid utopic struggling for an "ideal" horn or compression driver in attempt to minimize distortion below the level determined by the fundamental physical constraints. This concerns primarily air distortion causing deterioration of sound pressure signal in compression chamber and propagation distortion either in a horn or in a free space.

Modeling is only an attempt to simulate real physical effects, which are almost always more complex than a model that is confined within the boundaries of physical interpretation and mathematical apparatus. In this work the modeling methods were based primarily on solution of ordinary nonlinear differential equations. Correspondingly, the description of nonlinear distortion in compression driver was formulated in terms of solution of these equations. This does not cover the distributed mechanical and acoustical nonlinear effects such as the high frequency nonlinear resonances of air in the compression chamber, and nonlinear breakups of compression driver's diaphragm. These problems, difficult to solve, should be handled by different approaches involving solution of nonlinear partial differential equations, a vast and sophisticated area of mathematics and physics in its own right. Nevertheless, even without using this involved mathematical apparatus, plenty of useful information about nonlinear behavior of horn driver can be obtained through comparatively simple methods used in this work. Such information, presented as graphs of simulated distortion and as samples of distorted musical signal, is useful for an engineer and a researcher. This information helps to assess the influence of separate nonlinear mechanisms, gives a chance to obviate simplistic explanations, and helps to avoid erroneous allusions to various mysterious causes of sound deterioration.

Previous models of compression driver took into account nonlinear compression in the air chamber, but were either based on the use of simple sinusoidal input signal which prevented the prediction of reaction to more adequate complex signals such as multitone or band-limited noise, or they were based on application of Volterra expansion not capable of handling strong nonlinearity. The use of straightforward numerical solution of differential equations describing behavior of a compression driver was prevented by the fact the compression driver is loaded by the complex acoustical impedance of the phasing plug extending into the horn. This impedance is a complex function of a frequency that

does not belong in general to the class of fractional-rational functions, and therefore can not be transformed directly into time domain in the form of differential equations relating the pressure in compression chamber and particle velocity at the entrance of the phasing plug. In this work a new original approach was developed. The impedance of the acoustical load was approximated by a fractional-rational function, and the latter was turned into the system of differential equations and incorporated into the major system of differential equations governing operation of compression driver. This approach opened the door to comparatively simple nonlinear dynamic model handling a wide class of input signals, including musical signals.

A new model of a horn takes into account reflections of fundamental signal from the mouth and assumes that the distortion products propagate along the horn without reflections. Such assumption, not being completely precise from the academic standpoint, gives a chance to build a flexible and comparatively simple model capable to accurately predict nonlinear and linear distortion in a horn above its cut-off frequency. The fact that the majority of mid and high frequency horns are used above their cut-off frequency makes this assumption quite legitimate. The full-fledged modeling of nonlinear distortion in horns would need solution of partial nonlinear differential equations. Again, extending the well-known matrix method of horn linear modeling into nonlinear domain obviated this problem. The matrix calculations, Fourier transform, and numerical solution of algebraic implicit equations substituted solution of nonlinear partial differential equations. This approach significantly simplified the mathematical apparatus used for modeling and made it possible to model transformation of different signals.

The modeling and measurement of a particular compression driver illustrated the share of various nonlinear effects in horn driver. The nonlinear compression in the compression chamber was not the primary source of nonlinearity, whereas the propagation distortion from the horn's mouth to the microphone was quite comparable in level with distortion generated in the horn driver. The level of measured distortion is higher than that of the modeled distortion, which is indicative of "undermodeling". In other words, some of the nonlinear effects were not taken into account by the model at current stage. Some of these effects can be taken into account comparatively easy, at least it would not require radical changes in the model. Meanwhile, some of the nonlinear effects such as nonlinear breakups of the diaphragm need much more sophisticated approach based on numerical solution of nonlinear partial differential equations.

ACKNOWLEDGEMENT

The author would like to thank Gene Czerwinski for support. Many thanks go to Alex Terekhov and Sergei Alexandrov for their notes and suggestions and invaluable help in preparing this work for publication and presentation. The author is indebted to Dr. Yuri Il'inski from Texas University at Austin for enlightening discussions.

REFERENCES

[1] H. Schurer, A. Berkoff, "Modeling and Compensation of Nonlinear Distortion in Horn Loudspeakers", presented at the 96th AES Convention, Amsterdam, 1994, preprint 3819 (P7.5).

[2] P. Robineau, R. Vaucher, "Analysis of Nonlinear Distortion in Compression Drivers", presented at the 98th AES Convention, Paris, 1995, preprint 3998 (L4).

[3] A. Voishvillo, M. Olyushin, "Computer Modeling of Air Distortion in Compression Chamber of Horn Drivers with Centrally Supported Diaphragm", presented at the 99th AES Convention, New York, 1995, preprint 4062 (E-5).

[4] W. Klippel, "Nonlinear System Models for Horn Loudspeakers", presented at the 99th AES Convention, New York, 1995, preprint 4083 (I-5).

[5] W. Klippel, "Filter Structures to Compensate for Nonlinear Distortions of Horn Loudspeakers", presented at the 99th AES Convention, New York, 1995, preprint 4102 (L-8).

[6] P. Béquin, C. Morfey , "Weak Nonlinear Propagation of Sound in a Finite Exponential Horn", JASA, Vol. 109 (6), June 2001, pp. 2649 - 2659

[7] S. Billings, S. Fakhouri, "Nonlinear System Identification Using the Hammerstein Model", Int. J. Systems Sci. Vol. 10(5), June 1979, pp. 567 – 578.

[8] W. Klippel, "Nonlinear Wave Propagation in Horns and Ducts", JASA, Vol. 98, 1995, pp. 431 – 436.

[9] K. Holland, F. Fahy, C. Morfey, "Prediction and Measurement of the One-parameter Behavior of Horns", JAES, Vol. 39, No. 5, May 1991, pp. 315 – 337.

[10] D. Mapes-Riordan, "Horn Modeling with Conical and Cylindrical Transmission-Line Elements", JAES, Vol. 41, No. 6, June 1993, pp. 471 – 484.

[11] E. Czerwinski, A. Voishvillo, S. Alexandrov, A. Terekhov, "Multitone Testing of Sound System Components – Some Results and Conclusions" part 1, JAES, Vol. 49, No. 11, November 2001 pp. 1011-1048, part 2, JAES, Vol. 49, No 12, December 2001

[12] J. Buckman, "Distortion from Boundary Layers", presented at the 103rd AES Convention, New York, September 1997, preprint 4619 (B-10).

[13] W. Press, S. Teukolsky, W. Vettering, B. Flannery, "Numerical Recipies in C", Cambridge University Press, 1995.